LETTERS

Small vertical movement of a K^+ channel voltage sensor measured with luminescence energy transfer

David J. Posson[1], Pinghua Ge[1], Christopher Miller[2], Francisco Bezanilla[3] & Paul R. Selvin[1]

Voltage-gated ion channels open and close in response to voltage changes across electrically excitable cell membranes[1]. Voltage-gated potassium (Kv) channels are homotetramers with each subunit constructed from six transmembrane segments, S1–S6 (ref. 2). The voltage-sensing domain (segments S1–S4) contains charged arginine residues on S4 that move across the membrane electric field[2,3], modulating channel open probability. Understanding the physical movements of this voltage sensor is of fundamental importance and is the subject of controversy. Recently, the crystal structure of the KvAP[4] channel motivated an unconventional 'paddle model' of S4 charge movement, indicating that the segments S3b and S4 might move as a unit through the lipid bilayer with a large (15–20-Å) transmembrane displacement[5]. Here we show that the voltage-sensor segments do not undergo significant transmembrane translation. We tested the movement of these segments in functional *Shaker* K^+ channels by using luminescence resonance energy transfer to measure distances between the voltage sensors and a pore-bound scorpion toxin. Our results are consistent with a 2-Å vertical displacement of S4, not the large excursion predicted by the paddle model. This small movement supports an alternative model in which the protein shapes the electric field profile, focusing it across a narrow region of S4 (ref. 6).

Conformational changes in proteins can be studied in great detail by using fluorescence energy transfer as a spectroscopic ruler[7,8]. Luminescence resonance energy transfer (LRET) is a modified version that employs a lanthanide donor complex with a long excited-state lifetime[9,10]. This unconventional probe can donate energy to a conventional fluorescent acceptor in the standard distance-dependent manner of Förster theory[10], and energy transfer efficiency and distances are calculated from the time constants of acceptor fluorescence emission (see Methods). LRET is capable of accurately measuring distances on *Shaker* channels *in vivo* because only donor–acceptor pairs produce sensitized acceptor emission, which is measured after a brief time-gate rejects fast background fluorescence. Further advantages arise from the minimal spectral overlap of donor and acceptor, the zero intrinsic anisotropy of the donor lanthanide[11], and the accuracy with which donor quantum yield[10] and R_o (the characteristic distance of 50% energy transfer) can be estimated.

Gating-driven protein movements have previously been measured on the *Shaker* channel by using LRET[12] and conventional fluorescence resonance energy transfer[13] with both the donor and the acceptor labelled at sites on the voltage-sensing domains. This configuration measured distance changes parallel to the membrane between S4 helices in the same tetrameric channel but did not directly measure transmembrane movements. Here we have attached the acceptor dye to the channel by means of a scorpion toxin that binds to the pore from the external solution[14,15]. Toxin binding is insensitive to the channel's open or closed status and does not alter the movement of the voltage sensor[15,16]. Lanthanide donors were attached to several sites on S4, S3b and the S3–S4 linker region near S4, to test directly *in vivo* whether the voltage-sensing segments undergo a large transmembrane movement (Fig. 1). Any paddle-type mechanism by definition requires a transmembrane movement of 15–20 Å (ref. 5), equivalent to a change in distance of about 10 Å from S4 to toxin in the configuration used here, as estimated from conservative structural assumptions (Fig. 1). Testing the vertical translation of S3b–S4 is of central importance in evaluating the validity of the paddle mechanism, because the model's other unusual feature, the location of S4 at the lipid interface, has been shown experimentally to be plausible[17,18].

For LRET, ionic currents of *Shaker* expressed in *Xenopus* oocytes were blocked with 100 nM fluorescent charybdotoxin (CTX) or agitoxin-2 (AgTX) such that almost all channels were blocked and residual unblocked current was limited to 10–30 μA to minimize voltage-clamping errors[19]. The charge–voltage relations for donor-labelled channels were measured separately from cells blocked with a saturating level of unlabelled toxin (see Supplementary Information). Lanthanide-chelate donors (terbium) were attached to site-directed cysteine residues on the voltage-sensor domain (see Methods). The labelling of voltage-sensing segments with fluorescent probes does not disrupt the movement of gating charge. The effect of fluorescein (and rhodamine) was tested, but not terbium-chelate (see Supplementary Information). Toxin binding brought acceptor fluorophores into proximity to the labelled donor sites on the channel,

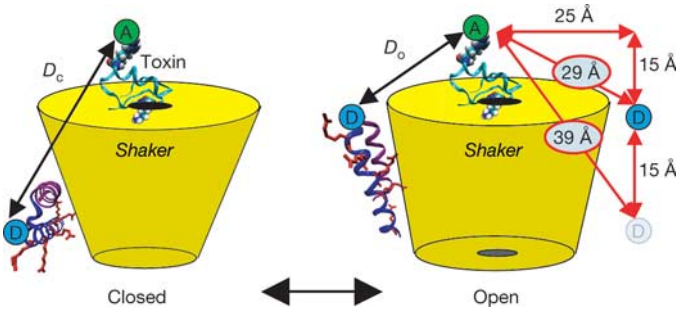

Figure 1 | Diagram of the paddle model. LRET measures distances from donor labelled sites (blue circles) on the S3b–S4 paddle (structure taken from the isolated voltage sensor[4]). The voltage-sensing arginine residues are shown in red. The energy-transfer acceptors (green circles) are attached to the top of the channel with a scorpion toxin. The paddle model predicts a change in distance, $D_c - D_o$, of 10 Å, estimated by a conservative geometric calculation assuming a 15-Å vertical translation (red arrows).

[1]Department of Physics and Biophysics Center, University of Illinois at Urbana-Champaign, Urbana, Illinois 61801, USA. [2]Department of Biochemistry, Howard Hughes Medical Institute, Brandeis University, Waltham, Massachusetts 02454, USA. [3]Department of Physiology and Department of Anesthesiology, UCLA School of Medicine, Los Angeles, California 90095, USA.

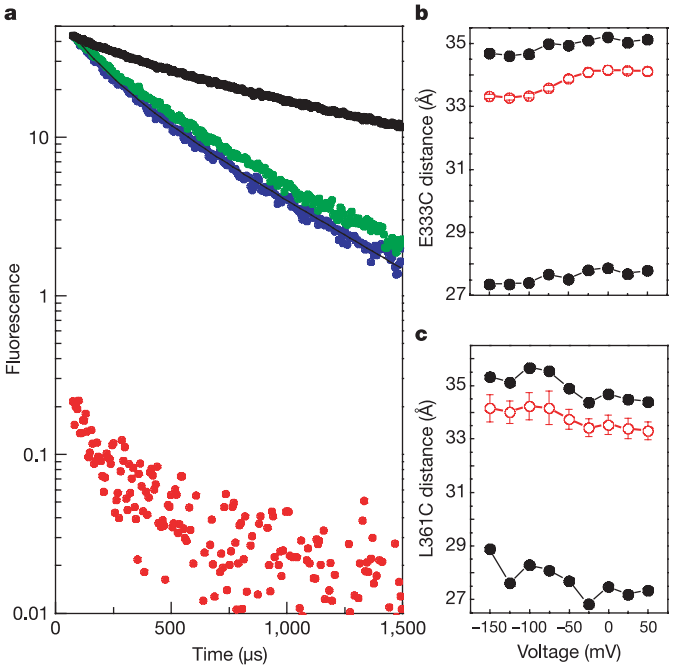

Figure 2 | LRET raw data and distance calculations. **a**, Acceptor-sensitized emission at two extreme voltages is shown for the E333C mutant near the top of the paddle. Black, donor only ($\tau_D = 1{,}600\,\mu s$); green, acceptor +50 mV; blue, acceptor −150 mV ($\tau_{AD} = 160\,\mu s$, 509 μs); red, average control data ($n = 6$). **b**, The time constants displayed a small voltage dependence corresponding to a small movement 0.8 Å away from the toxin. The distances calculated from the two lifetime components (black) and the weighted average (red; see Methods) are shown. **c**, L361C showed voltage-dependent movement of 0.8 Å towards the toxin. Error bars on the average distance represent s.e.m. ($n = 13$ in **b**; $n = 8$ in **c**).

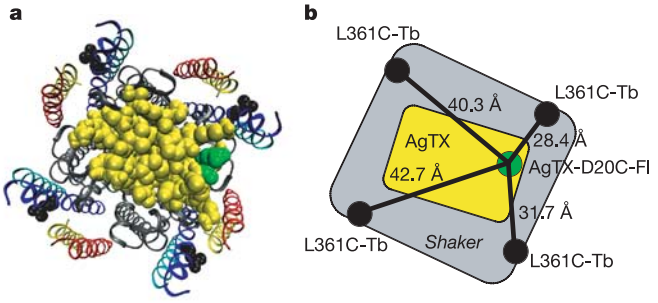

Figure 3 | A model of *Shaker* with docked AgTX predicts four distances for each LRET experiment. **a**, The coordinates provide an opportunity to compare our measurements with a picture of *Shaker* that has S3 and S4 placed against the pore domain. **b**, Distances for L361C on S4, measured from α-carbons.

and the distances were calculated as a function of voltage from the measured LRET time constants. Acceptor-sensitized emission data from E333C on S3b and background controls (see Methods) are shown in Fig. 2. LRET signals fitted well to two time constants that reflect the asymmetry of the toxin–acceptor position with respect to the central axis of the channel (Fig. 3). Distances from both time constants were calculated, as was a population-weighted average distance versus voltage (see Methods). These distances are shown for E333C on S3b and L361C on S4 (Fig. 2). The results show that sites homologous to the KvAP voltage-sensor paddle move less than 1 Å with respect to the toxin when going from the closed to the open channel positions. If the S4 segment moves in a purely vertical direction, a change in LRET distance of 1 Å corresponds to a 2 Å vertical displacement, as estimated by a conservative geometric calculation similar to that shown in Fig. 1.

Small but unambiguous voltage-dependent movements were seen at many sites (Fig. 4), with S3 moving about 1 Å away from the toxin, S4 moving about 1 Å towards the toxin, and the sites in the linker moving up to 2.5 Å in a manner consistent with a change in linker tilt[12]. We note that S3b and S4 move in opposite directions, instead of translating together as a rigid unit. For three sites, N353C, E335C and L361C, both AgTX and CTX gave similar calculated distances. Two sites on the S3–S4 linker were studied with two different acceptors, CTX-Lucifer Yellow and CTX-Atto465, which are useful for measuring distances as short as 15 Å (see Methods). For S346C, the calculated distances differed by only 2.5 Å, which may be attributed to differences in dye size and linker lengths. For S351C the distances obtained using CTX-Atto465 and CTX-4,4-difluoro-4-bora-3a,4a-diaza-*s*-indacene (BODIPY) Fl differed by 5 Å, but the gating-induced change in distance was unaffected by the choice of acceptor. Thus, the absolute distances are slightly uncertain, but the changes in distance are reproducible. As a further control, we switched the donor and acceptor for one experiment, labelling E333C with fluorescein acceptors and attaching a CTX-Tb donor to the top of the channel. The resulting distance measurements were nearly identical to those in Fig. 2 (see Supplementary Information). In every experiment, minimal voltage-dependent changes in both LRET amplitudes and time constants showed that only small changes in energy transfer occurred. These small changes refute the most central feature of the paddle model: substantial physical movement of gating charge transverse to the membrane plane.

We are confident that this LRET technique estimates distances faithfully, on proteins in general and in K^+ channels in particular. Beyond the technique's agreement with known structures in soluble proteins[10], distances measured here agree well with independent estimates of distances from the *Shaker* voltage sensors to the pore made with the use of tethered tetraethylammonium blockers[20]. For example, in the tether experiments, Q348C, D349C and K350C were found to be 17–18 Å from the pore in the open state, very similar to our measurements of 17–19 Å and 21–25 Å for S3–S4 linker residues S346C and S351C, respectively. Similarly, E334C and E335C were found to be about 30 Å from the pore in the tether experiments, close to our measurements for these same residues at the end of S3b, 32–34 Å. Although tethered blockers and LRET measure distances to two different points near the central pore, the close agreement between the approaches shows their power for constraining structural distances on the *Shaker* channel. Furthermore, tethered blockers measure distances only for the open state whereas LRET has the advantage of probing both open and closed states.

LRET measures absolute distances with less systematic error than traditional energy-transfer techniques[8,10] and can therefore be used to evaluate and constrain structural models. Recently, a structural model was proposed for the *Shaker* open state based on a combination of experimental data and molecular dynamics[21,22]. This model was supplemented with a computationally docked AgTX[23] so that theoretical distances from the toxin labelling site to sites on the

Table 1 | Comparison of LRET distance analysis with distances taken from a model of the *Shaker* open state

Donor site	Acceptor used	Average model *D* (Å)	Average simulation *D* (Å)	LRET average *D*
(S4) L361	BODIPY Fl-CTX	35.8	33.4	33.3
(S4) R365	BODIPY Fl-CTX	39.8	35.5	33.2
(S3b) V330	BODIPY Fl-CTX	30.9	30.2	34.8
(S3–S4 Linker) S351	BODIPY Fl-CTX	30.2	30.5	25.5
(S3–S4 Linker) S351	Atto465-CTX	30.2	25.0	21.0

Model *D* is the mean of four distances measured from the Cα of D20 on a docked AgTX to the Cα of specified sites on each subunit (Fig. 3). For simulation data see Methods and Supplementary Information.

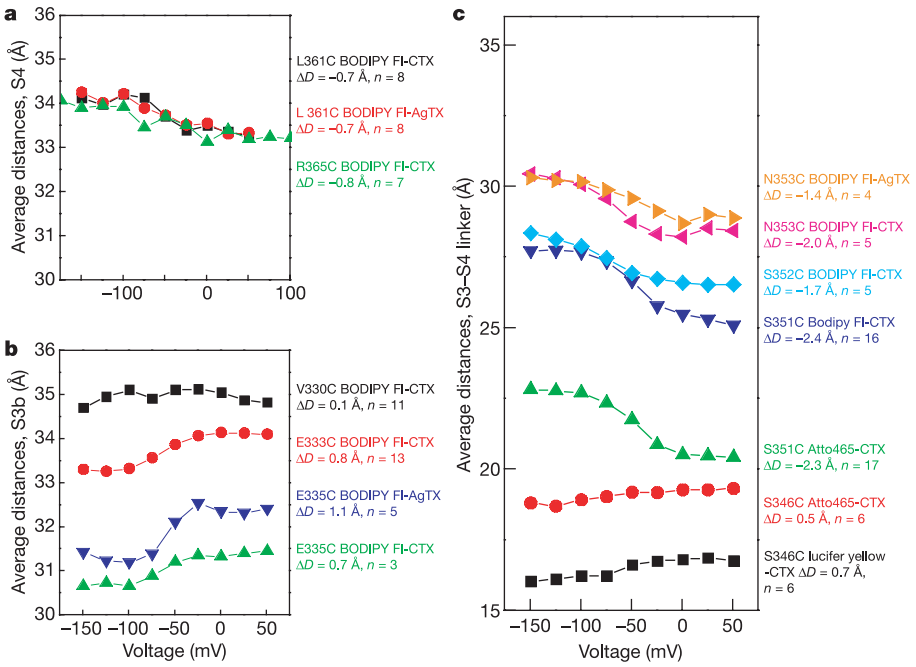

Figure 4 | Average distances for many *Shaker* sites. a, **b**, The S4 (**a**) and S3b (**b**) sites are homologous to sites on the KvAP voltage-sensing paddle. The distances for S4 change, 0.8 Å, consistent with a roughly 2-Å vertical translation. S3b moves in the direction opposite to S4, moving just 0.8 Å away from the toxin. **c**, Sites in the S3–S4 linker are clearly closer to the toxin than the transmembrane segments, as expected, and move no more than a few ångströms.

Shaker voltage sensor could be compared directly with our LRET measurements (Fig. 3). The model predicts four theoretical distances and we have used simulations to test how well LRET experiments can measure the average distance for situations of such geometric complexity (Table 1; see Methods and Supplementary Information). The simulations reproduce average distances in close agreement with model values; the exception was S351 using CTX-Atto465, for which the small R_o caused an underestimation. The LRET experimental results for two sites on S4 show very close agreement between model and data. However, the LRET measurements may systematically underestimate distances slightly because the position of the probes can wobble around their linker attachment points, weighting the measurement towards the distance of closest approach. The model prediction for S3b was unique in that it predicted a shorter distance (about 4 Å) than the distance measured experimentally. Nevertheless, the distance values obtained with LRET are consistent with the general structural view that S3 and S4 are transmembrane segments at all voltages.

The small vertical S4 movements presented here supplement the even smaller lateral movements between voltage sensors obtained previously[12] and indicate that the conformational changes underlying gating charge movement are subtle rather than substantial. The paddle model could be altered to account for our data by allowing the paddle segments to swing laterally outwards while undergoing vertical movement such that distances to the toxin remain constant. However, this kind of movement would be flatly inconsistent with the small lateral displacements observed in previous LRET measurements[12]. The small physical movements of voltage-sensing segments indicate that the membrane electric field must be focused over a very tight region of the voltage sensor, as if aqueous crevices penetrate the protein and thereby shape the field profile[6,24]. Small S4 movements relative to these crevices and voltage-induced changes in crevice shape can produce the large gating charge that must traverse the field to account for the steep voltage dependence of voltage-gated channels.

METHODS

Distance calculations. The lifetime of acceptor-sensitized emission was used to calculate energy transfer efficiency by using the relation $E = 1 - \tau_{AD}/\tau_D$, where τ_D is the lifetime of the donor in the absence of acceptor. τ_D was measured on channel sites in the absence of acceptors. On a few sites τ_D displayed a slight voltage dependence (S346C and S351C less than 10%; E335C less than 5%) and these changes were included in the analysis (distances changed were less than 1 Å). Sensitized emission data were fit to two exponentials using four parameters; A_1, τ_1, A_2, τ_2. Multiple time constants indicate that the acceptor molecule is not an equal distance from all four labelled donors to the voltage-sensing domains. An average lifetime was calculated by normalizing the sensitized emission lifetimes by the rate of energy transfer to obtain a 'population average'[25]

$$\bar{\tau} = \frac{(A_1/k_1)\tau_1 + (A_2/k_2)\tau_2}{(A_1/k_1) + (A_2/k_2)}$$

where $k_n = \tau_n^{-1} - \tau_D^{-1}$. Distances from τ_1, τ_2 and $\bar{\tau}$ were calculated by finding E (above) and using $R = R_o(E^{-1} - 1)^{1/6}$. Most data were taken by using BODIPY Fl-maleimide acceptors (Molecular Probes) for which $R_o = 39$ Å. Other data were taken with the use of Atto465-maleimide (Atto-Tec), $R_o = 27$ Å, and Lucifer Yellow-iodoacetamide (Molecular Probes), $R_o = 23$ Å.

Toxin biochemistry, *Shaker* expression and block. CTX-R19C and AgTX-D20C were prepared, labelled and purified as described previously[26]. The mass of each fluorescent toxin was verified by mass spectrometry, and high-affinity block with *Shaker* was evaluated qualitatively by examining the slow rate of toxin dissociation. The channel construct was the fast inactivation-removed, conducting *Shaker* H4IR, with the mutations F425G, K427D that increase the toxin binding to sub-nanomolar affinities[27]. *Xenopus* ooctye preparation, channel mutagenesis (Stratagene) and mRNA synthesis (Ambion) were performed with standard procedures. Experiments were performed typically 3–5 days after microinjection of 20 ng of *Shaker* mRNA. Voltage clamping was performed with a two-electrode setup (CA-1B; Dagan). Charge–voltage relations were measured with a saturating wild-type CTX block (2 μM), and LRET measurements were recorded with a nearly complete block with 100 nM fluorescent toxin (see Supplementary Information).

LRET protocols and controls. The optical setup consisted of an Olympus inverted IX-70 microscope with a 40 × quartz objective (numerical aperture 0.8; Partec). The lanthanide was excited with a pulsed 337-nm nitrogen laser source (Oriel), reflected by a 400DCLP dichroic filter (Chroma). Donor and acceptor

fluorescence were collected simultaneously with D490/10 and HQ520/20 filters, respectively (Chroma). Fluorescence was detected with two water-cooled R943-02 photomultiplier tubes (Hamamatsu) operated at −1,760 V. Prompt fluorescence was rejected by using an electronic gate (Products for Research) with a dead-time of 70 μs. The detector current was converted to voltage with a C7319 preamplifier (10^6 V/A; Hamamatsu) and filtered at 50 kHz (eight-pole Bessel filter; Dagan). The laser pulse was given exactly 40 ms after the initiation of a voltage step to ensure that the channels had reached conformational equilibrium before the LRET signals were measured.

Background cysteine residues on oocytes were generally prelabelled with β-maleimidopropionic acid (Sigma) for 1 h after a 2–3-day incubation at 12 °C to increase the specificity of donor labelling[28]. Oocytes were then incubated for 24–30 h at 18 °C to allow the surface expression of *Shaker*. Cells were placed in depolarizing solution for 30 min with 100 μM dithiothreitol to reduce cysteine thiols for reaction with maleimide. Dithiothreitol was washed away before the cells were placed in depolarizing solution containing 80 μM maleimide-lanthanide chelate. LRET signal to background was estimated for every LRET experiment by recording acceptor-sensitized emission signals from oocytes that were expressing high levels of the background *Shaker* construct without the experimental cysteine mutation. Controls were labelled identically to the LRET experiments.

LRET simulations with a *Shaker* model. Coordinates for the *Shaker* open-state model with docked AgTX[21,23] provide predictions for four different distances between the AgTX-D20 α-carbon and the four α-carbons of selected sites on the voltage sensors. Assuming these four distances, LRET signals were simulated by assuming a bi-exponential donor with a dominant component, 75% at 1,600 μs, and a minor component, 25% at 300 μs. The minor component adds a systematic error that slightly underestimates distances (less than 5%). The multiple components can be well described by fitting to two exponentials (see Supplementary Information), as were the experimental data. These calculations show how the complicated geometry of the model can be reduced to distance estimations in close agreement with actual LRET measurements (Table 1).

Received 6 March; accepted 18 May 2005.

1. Hodgkin, A. L. & Huxley, A. F. A quantitative description of membrane current and its application to conduction and excitation in nerve. *J. Physiol. (Lond.)* **117,** 500–544 (1952).
2. Bezanilla, F. The voltage sensor in voltage-dependent ion channels. *Physiol. Rev.* **80,** 555–592 (2000).
3. Armstrong, C. M. & Bezanilla, F. Currents related to movement of the gating particles of the sodium channels. *Nature* **242,** 459–461 (1973).
4. Jiang, Y. *et al.* X-ray structure of a voltage-dependent K^+ channel. *Nature* **423,** 33–41 (2003).
5. Jiang, Y., Ruta, V., Chen, J., Lee, A. & MacKinnon, R. The principle of gating charge movement in a voltage-dependent K^+ channel. *Nature* **423,** 42–48 (2003).
6. Starace, D. M. & Bezanilla, F. A proton pore in a potassium channel voltage sensor reveals a focused electric field. *Nature* **427,** 548–553 (2004).
7. Clegg, R. M. Fluorescence resonance energy transfer. *Curr. Opin. Biotechnol.* **6,** 103–110 (1995).
8. Selvin, P. R. The renaissance in fluorescence resonance energy transfer. *Nature Struct. Biol.* **7,** 730–734 (2000).
9. Selvin, P. R., Rana, T. M. & Hearst, J. E. Luminescence resonance energy transfer. *J. Am. Chem. Soc.* **116,** 6029–6030 (1994).
10. Selvin, P. R. Principles and biophysical applications of luminescent lanthanide probes. *Annu. Rev. Biophys. Biomol. Struct.* **31,** 275–302 (2002).
11. Reifenberger, J. G., Snyder, G. E., Baym, G. & Selvin, P. R. Emission polarization of europium and terbium chelates. *J. Phys. Chem. B* **107,** 12862–12873 (2003).
12. Cha, A., Snyder, G. E., Selvin, P. R. & Bezanilla, F. Atomic scale movement of the voltage sensing region in a potassium channel measured via spectroscopy. *Nature* **402,** 809–813 (1999).
13. Glauner, K. S., Mannuzzu, L. M., Gandhi, C. S. & Isacoff, E. Y. Spectroscopic mapping of voltage sensor movement in the Shaker potassium channel. *Nature* **402,** 813–817 (1999).
14. MacKinnon, R. & Miller, C. Mechanism of charybdotoxin block of the high-conductance, Ca^{2+}-activated K^+ channel. *J. Gen. Physiol.* **91,** 335–349 (1988).
15. Goldstein, S. A. & Miller, C. Mechanism of charybdotoxin block of a voltage-gated K^+ channel. *Biophys. J.* **65,** 1613–1619 (1993).
16. Aggarwal, S. K. & MacKinnon, R. Contribution of the S4 segment to gating charge in the Shaker K^+ channel. *Neuron* **16,** 1169–1177 (1996).
17. Hessa, T., White, S. H. & von Heijne, G. Membrane insertion of a potassium-channel voltage sensor. *Science* **307,** 1427 (2005).
18. Cuello, L. G., Cortes, D. M. & Perozo, E. Molecular architecture of the KvAP voltage-dependent K^+ channel in a lipid bilayer. *Science* **306,** 491–495 (2004).
19. Baumgartner, W., Islas, L. & Sigworth, F. J. Two-microelectrode voltage clamp of *Xenopus* oocytes: voltage errors and compensation for local current flow. *Biophys. J.* **77,** 1980–1991 (1999).
20. Blaustein, R. O., Cole, P. A., Williams, C. & Miller, C. Tethered blockers as molecular 'tape measures' for a voltage-gated K^+ channel. *Nature Struct. Biol.* **7,** 309–311 (2000).
21. Laine, M. *et al.* Atomic proximity between S4 segment and pore domain in Shaker potassium channels. *Neuron* **39,** 467–481 (2003).
22. Laine, M., Papazian, D. M. & Roux, B. Critical assessment of a proposed model of Shaker. *FEBS Lett.* **564,** 257–263 (2004).
23. Eriksson, M. A. & Roux, B. Modeling the structure of agitoxin in complex with the Shaker K^+ channel: a computational approach based on experimental distance restraints extracted from thermodynamic mutant cycles. *Biophys. J.* **83,** 2595–2609 (2002).
24. Asamoah, O. K., Wuskell, J. P., Loew, L. M. & Bezanilla, F. A fluorometric approach to local electric field measurements in a voltage-gated ion channel. *Neuron* **37,** 85–97 (2003).
25. Heyduk, T. & Heyduk, E. Luminescence energy transfer with lanthanide chelates: interpretation of sensitized acceptor decay amplitudes. *Anal. Biochem.* **289,** 60–67 (2001).
26. Shimony, E., Sun, T., Kolmakova-Partensky, L. & Miller, C. Engineering a uniquely reactive thiol into a cysteine-rich peptide. *Protein Eng.* **7,** 503–507 (1994).
27. Goldstein, S. A., Pheasant, D. J. & Miller, C. The charybdotoxin receptor of a Shaker K^+ channel: peptide and channel residues mediating molecular recognition. *Neuron* **12,** 1377–1388 (1994).
28. Mannuzzu, L. M., Moronne, M. M. & Isacoff, E. Y. Direct physical measure of conformational rearrangement underlying potassium channel gating. *Science* **271,** 213–216 (1996).

Supplementary Information is linked to the online version of the paper at www.nature.com/nature.

Acknowledgements We thank B. Roux for putting together coordinates for a combined model of the AgTX–*Shaker* complex[23] with the model for the *Shaker* open state[21], and L. Kolmakova-Partensky and T. Lawrecki for technical assistance. This work was supported by grants from the NIH, NSF, the Carver Foundation and the Cottrell funds of the Research Corp to P.R.S., from an NIH grant to F.P., and from the Howard Hughes Medical Institute to C.M. P.R.S. also thanks J. Ackland, J. Stenehjem and the other members of the Sharp Rehabilitation Center of San Diego for their care, which made this study possible.

Author Information Reprints and permissions information is available at npg.nature.com/reprintsandpermissions. The authors declare no competing financial interests. Correspondence and requests for materials should be addressed to P.R.S. (selvin@uiuc.edu).